REVIEW
J Clin Neurol 2009;5:107-119

Print ISSN 1738-6586 / On-line ISSN 2005-5013
10.3988/jcn.2009.5.3.107

Multimodal MRI for Ischemic Stroke: From Acute Therapy to Preventive Strategies

Oh Young Bang, MD

Department of Neurology, Samsung Medical Center, Sungkyunkwan University School of Medicine, Seoul, Korea

Received January 5, 2009
Revised July 17, 2009
Accepted July 17, 2009

Correspondence
Oh Young Bang, MD
Department of Neurology,
Samsung Medical Center,
Sungkyunkwan University
School of Medicine, 50 Irwon-dong,
Gangnam-gu, Seoul 135-710, Korea
Tel +82-2-3410-3599
Fax +82-2-3410-0052
E-mail nmboy@unitel.co.kr

Background and Purpose Conventional therapies for ischemic stroke include thrombolytic therapy, prevention of inappropriate coagulation and thrombosis, and surgery to repair vascular abnormalities. Over 10 years have passed since the US Food and Drug Administration approved intravenous tissue plasminogen activator for use in acute stroke patients, but most major clinical trials have failed during the last 2 decades, including large clinical trials for secondary prevention and neuroprotection. These results suggest the presence of heterogeneity among stroke patients. Neuroimaging techniques now allow changes to be observed in patients from the acute to the recovery phase. The role of MRI in stroke evaluation and treatment is discussed herein.

Main Contents Three MRI strategies are discussed with relevant examples. First, the following MRI strategies for acute ischemic stroke are presented: diffusion-perfusion mismatch, deoxygenation (oxygen extraction and cerebral metabolic rate of oxygen), and blood-brain barrier permeability derangement in selected patients for recanalization therapy. Second, multimodal MRI for identifying stroke mechanisms and the specific causes of stroke (i.e., patent foramen ovale, infective endocarditis, and nonbacterial thrombotic endocarditis) are presented, followed by MRI strategies for prevention of recurrent stroke: plaque images and flow dynamics for carotid intervention.

Expectations The studies reviewed herein suggest that using MRI to improve the understanding of individual pathophysiologies will further promote the development of rational stroke therapies tailored to the specifics of each case. **J Clin Neurol 2009;5:107-119**

Key Words atherosclerosis, stroke, perfusion, personalized treatment, MRI.

Introduction: Lessons from Recent Failures

Stroke is a leading cause of death, along with cancer and coronary heart disease, and is the most common cause of physical disabilities in adults. Conventional therapies for ischemic stroke include thrombolytic therapy, prevention of inappropriate coagulation and thrombosis, and surgery to repair vascular abnormalities. Over 10 years have passed since the US Food and Drug Administration approved intravenous tissue plasminogen activator (tPA) for use in acute stroke patients. Most major stroke trials have failed during the last 2 decades, including the following:

1) Large clinical trials of secondary prevention (enrolling up to tens of thousands of patients in each study), such as the Warfarin-Aspirin Symptomatic Intracranial Disease Study,[1] the Management of Atherothrombosis with Clopidogrel in High-Risk Patients with Recent Transient Ischemic Attack or Ischemic Stroke, and Clopidogrel for High Atherothrombotic Risk and Ischemic Stabilization, Management and Avoidance studies.[2]

2) Recent randomized trials of new thrombolysis agents, such as the Desmoteplase In Acute Ischemic Stroke (DIAS)-II and Abciximab in Emergent Stroke Treatment-II trials.[3]

3) Stroke Therapy Academic Industry Roundtable criteria-guided Neuroprotection Trial (NXY-059).[4]

These results indicate the need for measuring patient heterogeneity in stroke (i.e., individualization of the patient).[5] Unlike coronary heart disease, strokes are caused by numerous etiologies, including large-artery atherosclerosis, cardioembolism, and lacunar stroke. Neuroimaging techniques now allow changes to be observed in patients from the acute to

the recovery phase. The role of MRI in stroke evaluation and treatment is discussed herein.

MRI Imaging for the Acute Treatment of Ischemic Stroke

Brains in the general population, but not isolated cases

In the setting of acute ischemic stroke, arterial recanalization to restore antegrade perfusion to the ischemic territory remains the principal therapeutic approach. In the current era of evidence-based medicine, clinical benefit is measured by the number needed to treat (NNT).[6,7] It has been reported that the NNT for tPA to avert one case of dependence or death after stroke is 8.4.[8] In other words, for every 100 patients with acute stroke treated with tPA, approximately 32 have a better final outcome, 3 have a worse final outcome as a result of treatment,[9] and approximately 1 will experience a severely disabling or fatal outcome because of tPA-related symptomatic intracerebral hemorrhage.[10]

Evidence-based medicine requires standardized therapy rather than idiosyncrasy.[11] However, individual patient outcomes need to be considered in acute stroke for several reasons. First, individual hemodynamic characteristics are highly variable,[12] potentially reducing the validity of the NNT. Second, the few effective acute stroke treatments (including intravenous or intra-arterial fibrinolysis, and endovascular mechanical therapy) do not provide a gold-standard treatment. Last, but not least, the NNT is limited by the narrow indication for recanalization therapy ("not too late" and "not too large"), which is a relatively small percentage of the total population. The approval of tPA was based on the patient receiving it within 3 h of stroke symptom onset,[8] which limits the number of patients who can receive it.[13,14] Thus, stroke treatment represents an important opportunity for personalized medicine.

The "MRI-based" clock

Thrombolysis must be performed quickly because the benefit diminishes and the risk of bleeding increases as time elapses.[15,16] Until now, the time elapsed from the clinical onset of stroke to the start of treatment ("onset-to-treatment" clinical clock) has been an important concept in stroke treatment.[15] Efforts to administer tPA quickly have included education on stroke identification, telemedicine, and emergency room reorganization.[17,18]

Prior to attempted recanalization, the prediction of final infarct volume should recanalization not occur may facilitate candidate selection. Neuroimaging techniques have now provided the concept of the "MRI-based clock." MRI can provide information on tissue status (diffusion-restriction and hemodynamic compromise), anatomical aspects [integrity of the blood-brain barrier (BBB) and the site of vascular occlusion], and metabolic conditions (oxygen extraction and cerebral metabolic rate of oxygen), which allows the tailored application of recanalization therapy. These techniques could then increase the NNT and reduce the number needed to harm, expand the current narrow (<3 h) therapeutic window for acute stroke therapy, and enable more patients to be candidates for recanalization strategies.[19]

Diffusion-perfusion mismatching

Within minutes of an ischemic insult, a core region of tissue exhibits profound loss of blood flow and becomes irreversibly damage, even if blood flow is rapidly restored. However, the surrounding zone (penumbra) of moderate blood flow may still be rescued for several hours or more after symptom onset, and hence represents a suitable target for therapy.

The most common technique for imaging the ischemic penumbra in acute ischemic stroke patients is combined diffusion-weighted imaging (DWI) and perfusion-weighted imaging (PWI). DWI detects decreases in the self-diffusion of water molecules within minutes of onset; these changes are probably related to cellular energy failure and early cytotoxic edema, reflecting the physiologic consequences of ischemic injury. PWI provides a map of relative cerebral blood flow (CBF), permitting the identification of hypoperfused tissues. MRI characterization of the ischemic penumbra, as defined by the diffusion-perfusion mismatch, can delineate penumbral and irreversibly infarcted fields with a similar degree of reliability to the gold standard, positron-emission tomography (PET).[20] A significant diffusion-perfusion mismatch may be present up to 24 h or more after symptom onset, but mismatch volume progressively decreases over time.[21] The presence of a diffusion-perfusion mismatch could justify recanalization therapy beyond 3 h. For example, the phase II desmoteplase trials demonstrated that thrombolysis beyond 3 h works in patients with a significant penumbral area on pretreatment imaging.[22,23] Multiparametric MRI, including DWI and PWI, has increasingly been used in clinical practice,[24,25] although many uncertainties still exist.[26]

Patients Likely to Have a Favorable Clinical Response to Recanalization Therapy

In a prospective, multicenter study, pretreatment MRI could be used to differentiate between subgroups of stroke patients likely to benefit from reperfusion therapies given 3-6 h after stroke onset.[27] The study also provided a simple but valuable

MRI categorization strategy with profiles that are strongly associated with clinical outcomes after reperfusion therapy (i.e., mismatched vs. matched vs. small vs. malignant). Using 30-day fluid-attenuated inversion recovery (FLAIR) images, the Diffusion-weighted Imaging Evaluation For Understanding Stroke Evolution (DEFUSE) trial group reported a significant association between recanalization and reduced infarct growth in patients with mismatch who were treated with tPA within 3-6 hours after stroke onset.[28] Patients who exhibited a target mismatch pattern had a favorable clinical response to recanalization therapy (Fig. 1). However, diffusion-perfusion mismatch is only one contributor to tissue fate, even when recanalization is complete.[29]

Two variables characterize the extent of hypoperfusion: the volume of hypoperfused tissue and the intensity or severity of hypoperfusion within these regions.[27] Most studies have focused on the extent of hypoperfusion. The hemodynamic effects of the collateral circulation are important in maintaining perfusion in the penumbral regions.[30] Using pretreatment angiographic and MRI data in acute stroke patients, we have shown that pretreatment collaterals may influence the severity of ischemic injury over the hypoperfused region.[29] Patients with good collaterals had larger areas of mildly hypoperfused tissue than those with poor collaterals,[29] and infarct growth within the penumbral zone was smaller when collaterals were better, irrespective of the degree of recanalization.[29,31]

The collateral supply can be visualized using a dedicated MRI method (subtracting the image of the first movement map).[32] We found that, compared to the large cortical DWI pattern, the deep-infarcts pattern exhibited less severe hypoperfusion related to good collateral flows.[33] In addition, the perfusion status may largely depend on the stroke subtype; stroke patients with large intracranial atherosclerosis had different mismatch profiles, which were related to better collaterals, compared to other subtypes.[34]

The penumbra area is defined as a region of hypoperfusion but with some remaining metabolic activity. Thus, metabolic conditions such as the oxygen extraction fraction (OEF) and

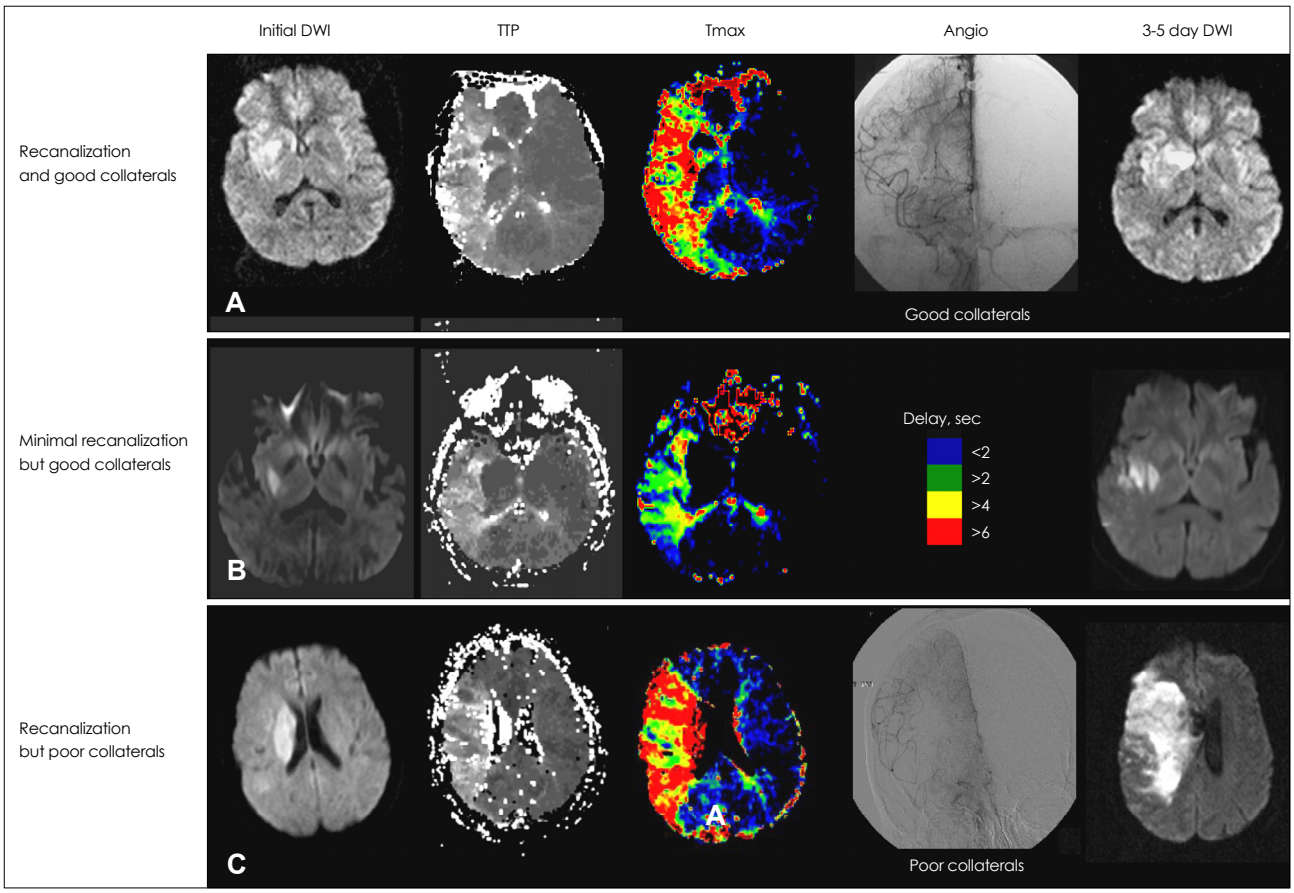

Fig. 1. Pretreatment DWI and PWI findings and final DWI findings of three patients with the target mismatch pattern (a PWI lesion that was ≥10 mL and ≥120% of the DWI lesion). A: Patients showing a favorable clinical response and no infarct growth after complete recanalization. B: Patients with good collaterals, showing minimal or no marked infarct growth after recanalization. C: Infarct growth was observed in patients with poor recanalization, despite recanalization. Figure modified from Bang et al.[29] DWI: diffusion-weighted imaging, PWI: perfusion-weighted imaging, TTP: time to peak.

the cerebral metabolic rate of oxygen also influence tissue fate after recanalization. Metabolic conditions in the ischemic penumbra may be predicted more accurately than simple diffusion-perfusion mismatch (which frequently overestimates the final lesion). They can enable visualization of the area of stage II hemodynamic failure (increased OEF).[35] Although PET measurement of cerebral blood volume (CBV), CBF, OEF, and regional cerebral metabolic rate of oxygen can identify stage II hemodynamic failure, its clinical use is limited, especially in acute stroke settings. MRI can detect misery perfusion (increased brain OEF in an area with reduced CBF but preserved oxygen metabolism).[36,37] T2*-weighted gradient-echo (GRE) imaging can also assess brain tissue viability.[36,38-40] GRE imaging is extremely sensitive to magnetic field inhomogeneities, since acute decreases in GRE imaging occur in animal models and stroke patients due to blood deoxygenation and increased OEF.[36,41,42] The paramagnetic effect of deoxyhemoglobin produces blood-oxygen-level-dependent (BOLD) contrast.[43] OEF values from MRI and PET are generally consistent.[39] By applying either quantitative BOLD imaging[36,39,44] or directly demonstrating intravascular deoxygenation changes on T2*-weighted GRE imaging,[40,45] increased OEF can be measured as an increase in deoxyhemoglobin. These measures offer an estimation of the oxygen utilization and provide additional information concerning the metabolic state of the threatened brain.

Fig. 2 shows a case with prominent hypointense leptomeningeal vessels. Although mismatch areas showed an extensive, severe delay in time-dependent PWI [time to peak after deconvolution (T_{max}) delayed by 8 s or more], suggesting an ischemic core, increased CBV and GRE-hypointense vessels within the hypoperfused area suggested the presence of viable tissue.[36,39] CBV was increased in these areas, reflecting an efficient collateral blood flow soon after arterial occlusion, which may indicate the ability of ischemic tissue to compensate for a decreased CBF.[40] Hypointense vessels were correlated with a larger perfusion defect and a larger perfusion delay, but an increased CBV.[45] These hypointense

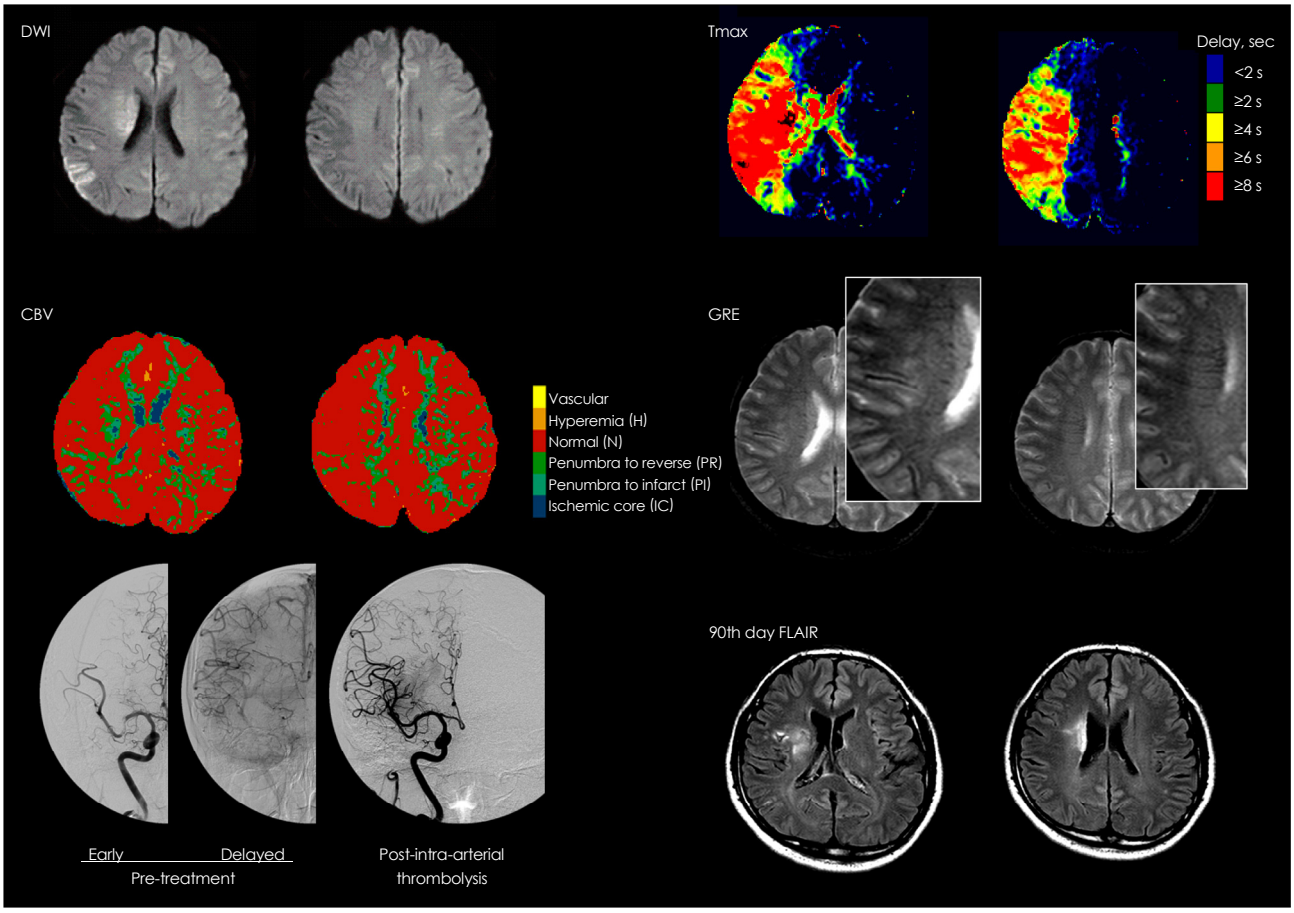

Fig. 2. DWI performed 4 h after symptom onset, disclosing multiple acute cortical and basal ganglia infarcts. A more extensive perfusion abnormality with mismatch was noted throughout the right middle cerebral artery (MCA) bed. However, CBV sustained the ischemic regions, and hypointense leptomeningeal and periventricular vessels were observed on GRE imaging. Recanalization with intra-arterial thrombolysis at 6 h resulted in complete reperfusion. No new lesions developed, as observed on the 90th day FLAIR imaging. Figure modified from Bang et al.[103] DWI: diffusion-weighted imaging, CBV: cerebral blood volume, GRE: gradient-echo, FLAIR: fluid-attenuated inversion recovery.

areas on GRE imaging became infarcted during the subacute and chronic phases.[36,46] Brain areas with hypointense signaling on GRE imaging may be targets for acute therapy to improve compromised cerebral circulation.[36] However, further validation of GRE imaging for assessing brain tissue viability is necessary, and it is limited by susceptibility artifacts.[38]

No parameters among CBV, CBF, mean transit time (MTT, first movement of the signal intensity curve), time to peak (TTP), and time to maximum tissue residue function (T_{max}, time to peak after deconvolution), is superior in predicting tissue fate after recanalization. The size of a perfusion lesion differs markedly depending on which of the ten PWI post-processing methods are used.[47] The time-domain perfusion parameters (e.g., MTT, TTP, and T_{max}) are being used increasingly in clinical practice, but may have considerable drawbacks in certain situations. For example, PWI may yield inconsistent data from time-dependent and nondependent domains; patients with severe delays in perfusion may a have preserved CBV (Fig. 2). Prominent dispersion and CBV preservation or augmentation might sustain the ischemic regions. A multiparameter approach has been suggested to help define the PWI abnormalities, by combining data from relative CBF, regional CBV, and time-domain maps.[48] In certain clinical settings of acute ischemic stroke with prominent collaterals at the time of PWI acquisition (such as populations in which intracranial occlusive disease is prevalent), time-domain PWI parameters may overestimate the perfusion severity and extent and should be interpreted with caution; a non-time-domain PWI parameter may be needed.[48]

Patients who are Unlikely to Exhibit a Favorable Clinical Response to Recanalization Therapy

Patients who do not exhibit mismatch patterns are unlikely to have a good clinical response to recanalization therapy, because it has been shown that in the presence of reperfusion, an increasing mismatch ratio was associated with a higher response rate (Fig. 3).[49] The DEFUSE trialists exhibited the current mismatch ratio of 1.2 to 1.8-2.6, although this may reduce the number of patients with mismatch (eligible for reperfusion therapy) by 15-25%.[49] Overestimation of the penumbra area may have contributed to the failure of the recent reported DIAS-II trial to document benefits of recanalization therapy in mismatch patients.[50] Thus, reperfusion in patients with a mismatch ratio below these cutoffs may have no beneficial effects, and may in fact be harmful. Further studies are needed to determine the optimal definition of a target mismatch pattern, as well as the mismatch ratio, PWI parameter, and each threshold.[26,50]

Hemorrhagic transformation (HT)-which is a much-feared complication of recanalization therapy for acute ischemic stroke-and hemorrhagic stroke can be visualized with high sensitivity and specificity. GRE imaging accentuates the paramagnetic properties of blood products such as deoxyhemoglobin, intracellular methemoglobin, and hemosiderin, and can detect hemorrhage and intravascular clots. A prospective multicenter trial has shown that GRE imaging is as accurate as CT at detecting acute hemorrhage in patients with acute

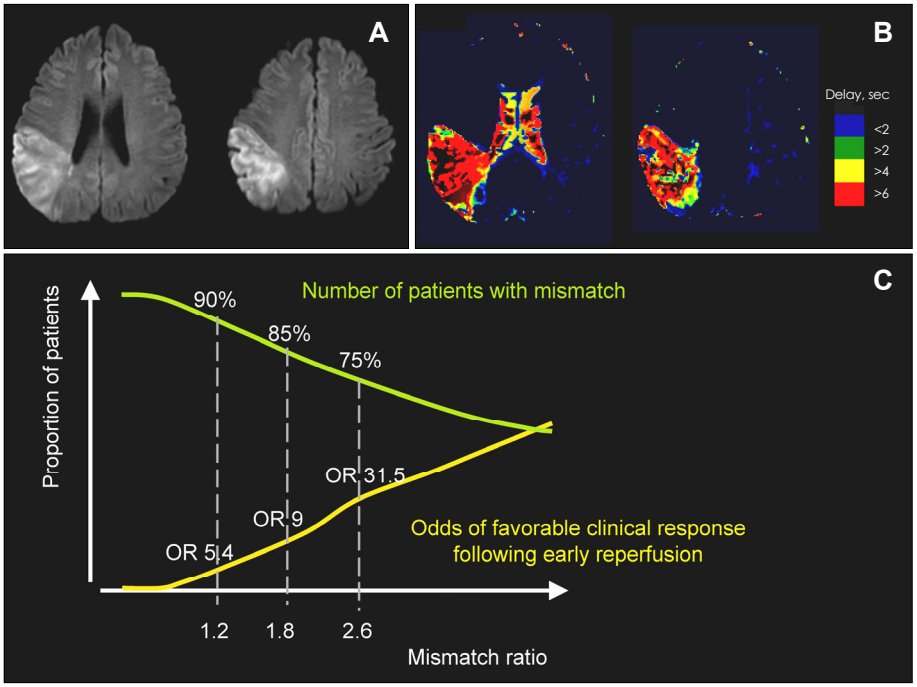

Fig. 3. DWI (A) and PWI (B) findings of a patient who exhibited the no-match pattern (a PWI volume <120% of the DWI lesion volume). The lesion was located on a relatively silent brain area. (C) Relationship between the number of patients with mismatch and the odds of a favorable clinical response following early reperfusion, and the mismatch ratio (the volume ratio of T_{max} ≥2 s over the DWI lesion).[49] DWI: diffusion-weighted imaging, PWI: perfusion-weighted imaging.

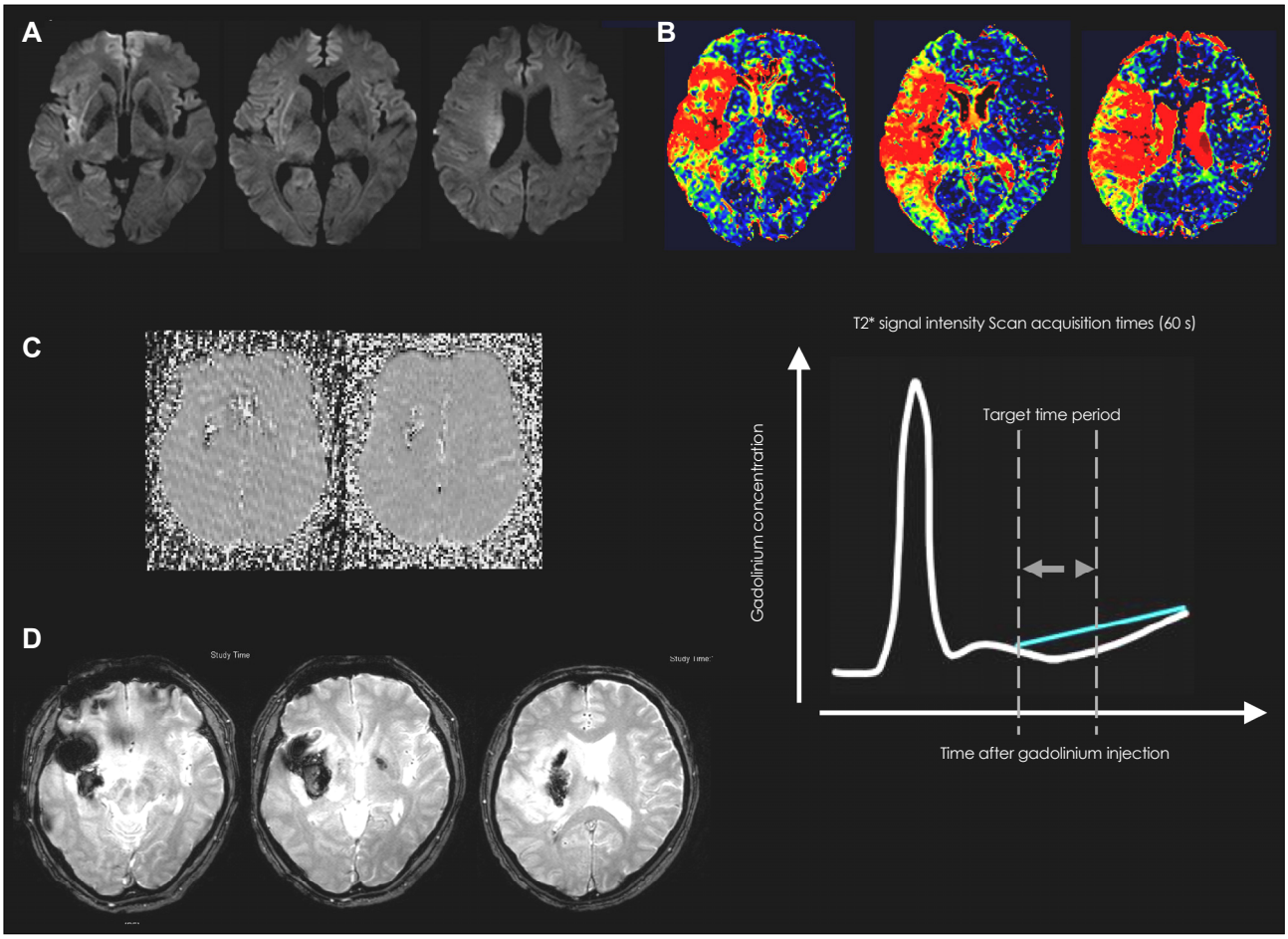

Fig. 4. A case showing the malignant profile on baseline MRI (a DWI lesion ≥100 mL and/or a PWI lesion of T_{max} delay ≥8 s and ≥100 mL). A: DWI performed 1 h after symptom onset, disclosing small acute cortical and basal ganglia infarcts. B: A more extensive perfusion abnormality with severe delay (T_{max} ≥8 s, >100 mL) was noted throughout the right MCA distribution. C: Pretreatment permeability slope image showing breakdown of the BBB. The white line delineates the slope of increasing Gd concentration after bolus passage and expected decreasing concentration during later times. The green line represents the slope of increasing Gd concentration during later times in patients with a dysfunctional BBB. Figure modified from Bang et al.[62] D: The patient showed clinical worsening with hemorrhagic transformation during follow-up. DWI: diffusion-weighted imaging, PWI: perfusion-weighted imaging, BBB: blood-brain barrier, MCA: middle cerebral artery, Gd: gadolinium.

stroke.[51]

Fig. 4 shows a case with HT, and demonstrates the relationship between the severity of tissue damage and the development of subsequent HT. A recent multicenter study found that the risk of symptomatic intracranial hemorrhage after thrombolytic therapy increased with increased DWI lesion volume.[52] The DEFUSE trial defined this malignant profile as extensive severe hypoperfusion with a large DWI lesion volume.[27] In that study, early reperfusion was associated with fatal intracranial hemorrhage in patients with a malignant profile.

There have been numerous efforts to predict HT using MRI. Diffusion-perfusion characterization of the ischemic territory may help identify patients at increased risk for HT after recanalization therapy: DWI lesion volume,[52] apparent diffusion coefficient (ADC),[53] and degree of hypoperfusion.[27,54] Additional MRI parameters may also reflect an increased risk for HT after thrombolysis: leukoaraiosis,[55] cerebral microbleeds, early parenchymal enhancement,[56] and early cerebrospinal fluid hyperintensity.[57]

BBB permeability dysfunction often precedes HT. Gadolinium (Gd) contrast agents are routinely used to detect BBB opening in patients with strokes or tumors, although routine Gd enhancement does not detect modest changes in BBB permeability. Suboptimal delivery of the contrast agent to the affected region due to a lowered CBF may result in these subtle changes in BBB permeability being missed.[58] Permeability assessment methods have shown permeability derangement in patients with ischemic stroke or malignant brain tumors,[59,60] and recently with ischemic stroke that could not be demonstrated by simple postcontrast spin-echo imaging alone.[61,62] We have applied a novel MRI permeability assess-

ment technique that employs perfusion scan source data to assess BBB dysfunction in acute ischemic stroke and evaluate the association between permeability changes and subsequent HT after recanalization therapy.[62] In this study, some degree of HT occurred in 12 of 32 patients. Permeability image abnormalities at baseline were present in 7 of 12 patients with HT and in none of 20 patients without HT on follow-up images. These preliminary data suggest that permeability images derived from pretreatment perfusion MRI data identify patients at risk of HT with high specificity. MRI guidance of interventional decision-making may be improved by supplementing standard penumbral imaging (indicating the potential to benefit from recanalization) with the use of slope imaging (which identifies individuals with BBB disruption who are at high risk of harmful treatment effects due to HT). Excluding patients at high risk of HT may improve the safety profile and risk: benefit ratio.

Permeability derangement is a dynamic process associated with ischemic stroke pathophysiology and recanalization therapy. Although disruption of the BBB is a necessary (albeit not sufficient) condition for intracerebral hemorrhage, it can be benign in certain conditions.[63,64] Even if BBB leakage is present, the patterns and destiny of permeability derangement vary. Moreover, predictors of permeability derangement may be different pre- and posttreatment.[64]

Finally, the clinical features and lesion site are also important; location may be more important than the volume of salvageable tissue. Patients with a similar infarct volume may show variable severity of neurologic deficits; some patients may have lesions in critical regions such as the corticospinal area, versus less critical areas such as the association cortex (e.g., the case presented in Fig. 3). The latter patients might not be candidates for potentially harmful recanalization therapy. Dr. Lev indicated the importance of "location-weight" scoring over simple volumetric data in penumbra areas.[65] Locating the mismatch before treatment may help to predict the potential benefits of reperfusion.[66]

Identification of Stroke Mechanisms

Multimodal MRI can identify the age and vascular territories involved in infarcts (Fig. 5). In most centers, the diagnosis of ischemic stroke subtype is performed during the first few days or weeks after hospitalization. Multimodal MRI, including DWI and magnetic resonance angiography (MRA), performed within a few hours of arrival at the hospital allows the rapid and accurate identification of early ischemic subtypes.[67,68] In particular, a cardioembolism can easily be esta-

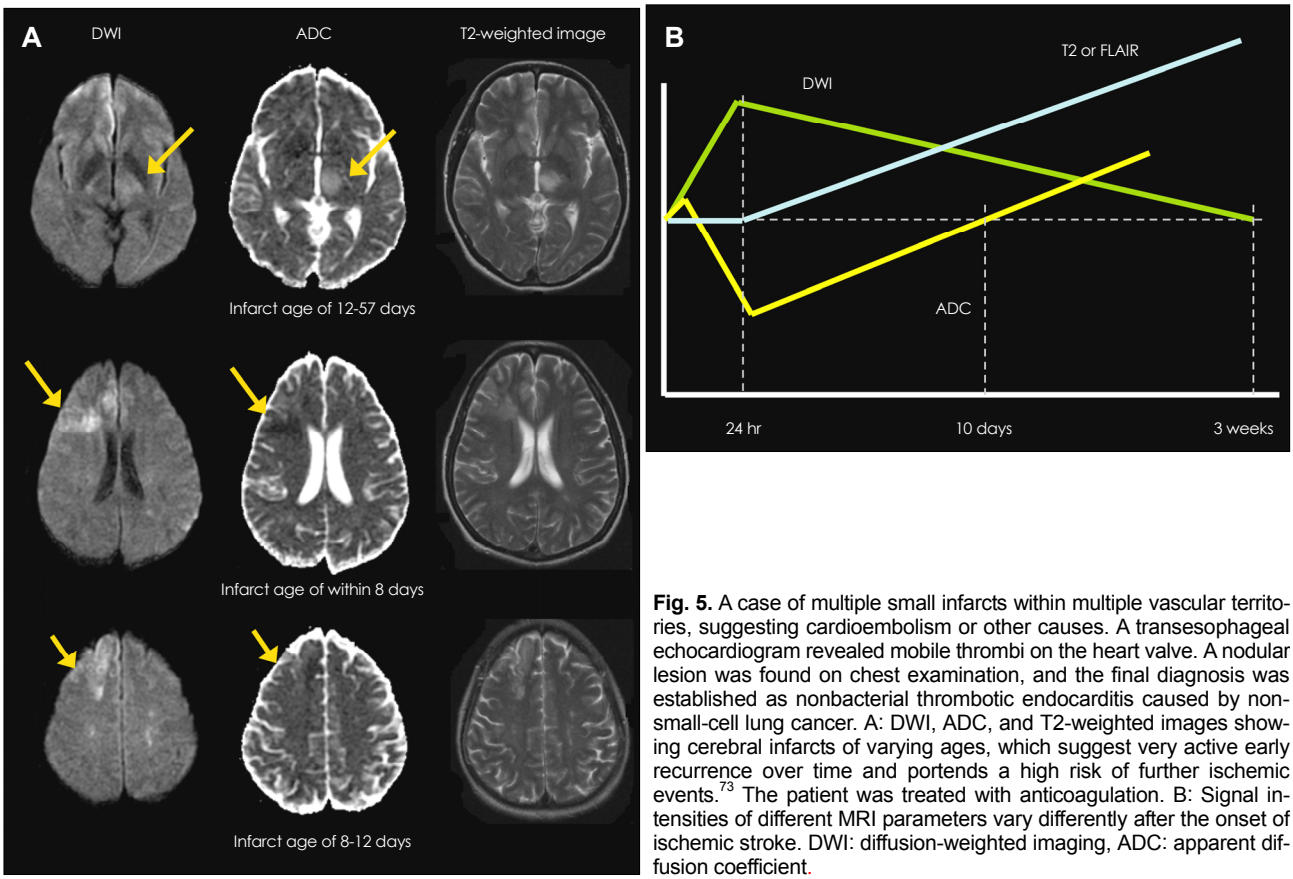

Fig. 5. A case of multiple small infarcts within multiple vascular territories, suggesting cardioembolism or other causes. A transesophageal echocardiogram revealed mobile thrombi on the heart valve. A nodular lesion was found on chest examination, and the final diagnosis was established as nonbacterial thrombotic endocarditis caused by non-small-cell lung cancer. A: DWI, ADC, and T2-weighted images showing cerebral infarcts of varying ages, which suggest very active early recurrence over time and portends a high risk of further ischemic events.[73] The patient was treated with anticoagulation. B: Signal intensities of different MRI parameters vary differently after the onset of ischemic stroke. DWI: diffusion-weighted imaging, ADC: apparent diffusion coefficient.

blished when patients exhibit acute lesions in multiple vascular territories, enabling the physician to consider early anticoagulant use.[67]

The infarct pattern on DWI is correlated with the pathogenic mechanisms underlying the stroke and may predict stroke recurrence and outcome.[69] Small acute lesions in multiple vascular beds on DWI provide insight into the stroke mechanism by predicting the proximal source of the embolism.[70,71] In addition, the ADC may be useful for estimating the lesion age and distinguishing acute from subacute DWI lesions.[72] Acute ischemic lesions can be divided into hyperacute lesions (low ADC and DWI-positive) and subacute lesions (normalized ADC). Chronic lesions can be differentiated from acute lesions by normalization of ADC and DWI. The presence of multiple DWI lesions of varying ages suggests active early recurrences over time and portends a higher early risk of future ischemic events.[73]

Multimodal MRI may also indicate stroke mechanisms. Silent cerebral microbleeds that are visible on T2*-weighted imaging may be seen as corticomeningeal microbleeds in patients with infective endocarditis,[74] enabling the provision of appropriate antimicrobial therapy and avoiding antithrombotic treatment, which could cause increased mortality. In contrast, it has been shown that patients with nonbacterial thrombotic endocarditis exhibit multiple disseminated infarctions of varying size, with at least one medium or large lesion on DWI.[75] Large thrombi that are fragile (i.e., lacking an inflammatory reaction and with little cellular organization) could underlie this DWI pattern, distinguishing it from infective endocarditis or cardioembolic stroke.[75] Finally, patent foramen ovale is a potential risk factor for ischemic stroke and shows different infarct patterns on DWI. Patients with patent foramen ovale showed embolic infarcts, especially multiple lesions in the posterior circulation,[76] which may reflect the finding of higher blood flow in the posterior circulation than the anterior circulation during the Valsalva maneuver.[77]

Small-vessel disease resulting from hypertension is the most common cause of stroke, and has characteristic clinical features and a good prognosis. DWI allows the detection of silent infarctions at different sites from the symptomatic, small, deep infarction, and concomitant small lesions outside the striatocapsular distribution could be identified. We have reported that proximal middle cerebral artery lesions are a common cause of small deep infarcts,[78] and that patients with parental arterial disease (by branch atherosclerosis) are more likely to have recurrent strokes and a poor long-term prognosis.[79] These results emphasize the importance of performing vascular studies in intracranial vessels, as indicated in Fig. 6.

The traditional criterion of an infarct size of <15 mm has recently been challenged.[80,81] The infarct size in patients with symptomatic small arterial occlusions varied from 3.1 to 38.7 mm.[81] A new stroke classification (Scandinavian Stroke Scale-Trial of Org 10172 in Acute Stroke Treatment)[82] that used an

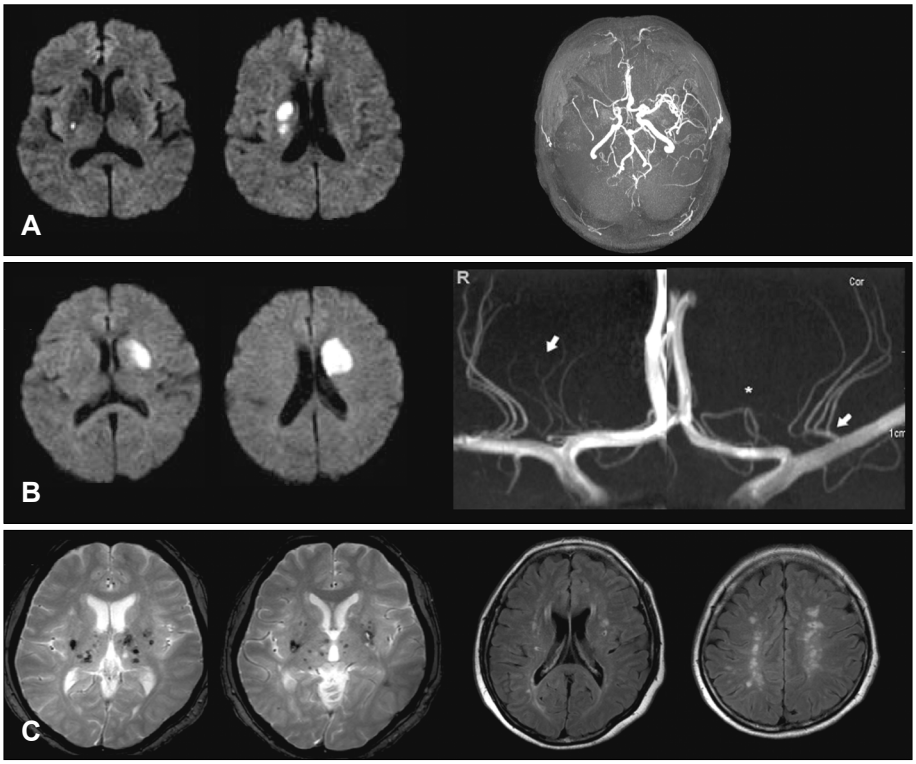

Fig. 6. Three cases with small, deep infarcts. A: Small, deep infarcts suggesting lacunar stroke, but MRA revealed MCA atherosclerosis, suggesting the presence of mural thrombi occluding the orifices of the lenticulostriate arteries. B: A relatively large, deep infarct but normal parent arteries, suggesting common trunk occlusion. High-resolution MRA (7.0 T) showing an example of four lenticulostriate arteries branching from a single trunk of the left MCA. Figure modified from Cho et al.[83] C: A patient with previous lacunar stroke who developed pseudobulbar palsy during aggressive antiplatelet and anticoagulation therapy. DWI was negative, but GRE imaging showed multiple microbleeds in the bilateral basal ganglia and thalamus, and periventricular leukoariosis. MCA: middle cerebral artery, MRA: magnetic resonance angiography, DWI: diffusion-weighted imaging, GRE: gradient-echo.

infarct size criterion of 20 mm rather than 15 mm was designed for the diagnosis of lacunar stroke. The large variation of infarct size may be related to the branching patterns of perforating arteries (Fig. 6); Cho et al.[83] recently showed an atypical branch pattern using high-resolution MRA.

It has been shown that recurrent intracranial hemorrhage is more frequent following lacunar vs. nonlacunar infarction.[84] Another study has shown that the prevalence of microbleeds was higher in lacunar stroke (62%) than in other infarct subtypes (21-30%),[85] which may be attributable to the increased risk of subsequent intracranial hemorrhage. These results suggest the importance of performing GRE imaging to avoid aggressive antithrombotic therapy and possible bleeding complications in patients with multiple microbleeds.

Stroke Prevention and Recovery

Atherosclerosis is an inflammatory disease. Coronary and carotid histology show that inflammatory cells such as macrophages mediate the development and progression of atherosclerosis. In addition, inflammatory markers such as C-reactive protein are associated with the progression of atherosclerosis and stroke recurrence. Vulnerable plaques typically have a substantial lipid core and a thin fibrous cap. Thrombotic coronary artery occlusion usually follows rupture of an unstable atherosclerotic plaque; the at-risk or vulnerable asymptomatic atherosclerotic coronary artery plaque is not associated with high-grade stenosis. Carotid atherosclerosis has many identical clinical and pathological features to coronary atherosclerosis.

Plaque vulnerability is identified by MRI[86] in three ways (Fig. 7): 1) multicontrast MRI, 2) commercially available nonspecific contrast agents, and 3) molecular imaging probes (for details see the review by Briley-Saebo et al.[86]). Multicontrast MRI characterizes the key structures (e.g., the lipid core, fibrous cap, and intraplaque hemorrhage) using signal variation after pulse sequences (with T1-, T2-, and proton-density-weighted images being the most commonly used) to identify plaque composition. MRI-based tissue quantification is accurate and reproducible; when compared with carotid endarterectomy specimens, *in vivo* multicontrast MRI could distinguish advanced lesions from earlier atherosclerotic plaques.[87,88] Commercially available nonspecific contrast agents (i.e., Gd-diethylenetriamine penta-acetic acid) can reveal plaque structures that are indicative of vulnerability (e.g., necrotic lipid cores and fibrous caps) and allow the assessment of plaque neovascularization.[86] Contrast agents that characterize thrombi are under development.[89,90]

Molecular imaging probes targeted to biochemical and/or cellular targets (such as macrophages, matrix metalloproteinase) can indicate plaque vulnerability.[86] Ultrasmall superparamagnetic particles of iron oxide (USPIO) are the best studied in stroke patients.[91,92] USPIO are nanoparticles of iron oxide that can be taken up by macrophages, thus decreasing

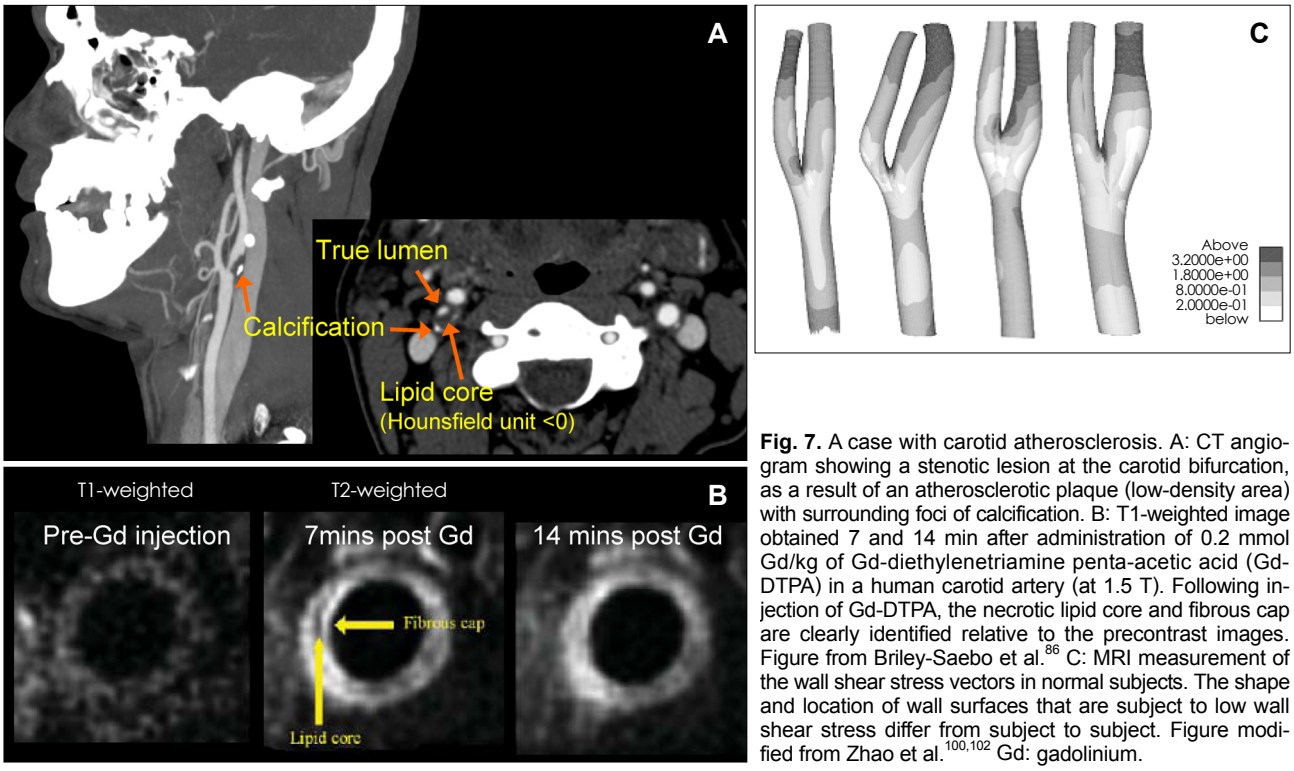

Fig. 7. A case with carotid atherosclerosis. A: CT angiogram showing a stenotic lesion at the carotid bifurcation, as a result of an atherosclerotic plaque (low-density area) with surrounding foci of calcification. B: T1-weighted image obtained 7 and 14 min after administration of 0.2 mmol Gd/kg of Gd-diethylenetriamine penta-acetic acid (Gd-DTPA) in a human carotid artery (at 1.5 T). Following injection of Gd-DTPA, the necrotic lipid core and fibrous cap are clearly identified relative to the precontrast images. Figure from Briley-Saebo et al.[86] C: MRI measurement of the wall shear stress vectors in normal subjects. The shape and location of wall surfaces that are subject to low wall shear stress differ from subject to subject. Figure modified from Zhao et al.[100,102] Gd: gadolinium.

the MRI signal. Macrophage accumulation in the carotid plaque can be visualized using GRE imaging (as a signal decrease in part of the vessel wall after USPIO administration).[91] Both histological analysis and MRI of symptomatic patients who have undergone carotid endarterectomy have shown that macrophage accumulation (shown by USPIO) was more prevalent in the ruptured and rupture-prone lesions than in the stable lesions.[91] Areas of reduced signal intensity were observed in 24 out of 27 patients (89%) with symptomatic carotid stenosis.[92]

Thrombogenicity is related to hemorheology (e.g., high shear stress, oscillatory shear stress, and local stasis) as well as local (i.e., plaque structure) or systemic (e.g., inflammation) conditions.[93-97] Clinical studies of intra-aneurysmal hemodynamics have shown that specific flow patterns may be related to risk of aneurysm rupture.[98] Similarly, the greatest atherosclerotic plaque accumulation typically occurs on the outer wall of the proximal segment of the sinus of the internal carotid artery, in the region with the lowest wall shear stress.[99] MRI can measure wall shear stress vectors in normal subjects or in patients with carotid atherosclerosis.[100,101] The shapes and locations of low-shear-stress wall surfaces differ between individuals,[100,102] which may explain why strokes recur in some patients and not in others. Although the degree of stenosis is the key factor to consider before intervention, patients with the same degree of stenosis on the carotid bifurcation or intracranial vessels do not have the same rate of progression of stenosis or stroke recurrence. Measurement of the role of flow pattern (i.e., wall shear stress and oscillation) on the development and progression of atherosclerosis using angiographic or noninvasive imaging merits further study.

The evaluation of changes in motor function can be achieved with functional MRI, diffusion tensor imaging, and molecular MRI. This research is outside the scope of the present review.

Conclusions

The American Stroke Association/American Heart Association Stroke Council has issued the statement that multimodal CT and MRI data may improve the diagnosis of ischemic stroke (class I, level A).[17] Using MRI techniques to understand individual case pathophysiologies will allow the future development of rational stroke therapies that are tailored to the specifics of each case. Measuring salvageable tissue and permeability derangements on MRI may help select patients for recanalization therapy.[104] MRI can also guide decision-making in stroke intervention, such as stenting and carotid endarterectomy, by providing information on plaque characteristics and the rheological aspects of atherosclerotic stenosis.

We are living in an era in which stroke physicians have difficulty keeping up with developments in imaging techniques. Multimodal MRI has significant potential for improving treatments and outcomes in stroke, as well as improving decision-making algorithms and estimates of the NNT or the number needed to harm.

Acknowledgements

This study was supported by a grant of the Korean Healthcare technology R&D Project, Ministry of Health & Welfare, Republic of Korea (A080044).

REFERENCES

1. Chimowitz MI, Lynn MJ, Howlett-Smith H, Stern BJ, Hertzberg VS, Frankel MR, et al. Comparison of warfarin and aspirin for symptomatic intracranial arterial stenosis. *N Engl J Med* 2005;352:1305-1316.
2. Bhatt DL, Fox KA, Hacke W, Berger PB, Black HR, Boden WE, et al. Clopidogrel and aspirin versus aspirin alone for the prevention of atherothrombotic events. *N Engl J Med* 2006;354:1706-1717.
3. Adams HP Jr, Effron MB, Torner J, Dávalos A, Frayne J, Teal P, et al. Emergency administration of abciximab for treatment of patients with acute ischemic stroke: results of an international phase III trial: Abciximab in Emergency Treatment of Stroke Trial (AbESTT-II). *Stroke* 2008;39:87-99.
4. Shuaib A, Lees KR, Lyden P, Grotta J, Davalos A, Davis SM, et al. NXY-059 for the treatment of acute ischemic stroke. *N Engl J Med* 2007;357:562-571.
5. Caplan LR. Evidence based medicine: concerns of a clinical neurologist. *J Neurol Neurosurg Psychiatry* 2001;71:569-574.
6. McAlister FA, Straus SE, Guyatt GH, Haynes RB. Users' guides to the medical literature: XX. Integrating research evidence with the care of the individual patient. Evidence-Based Medicine Working Group. *JAMA* 2000;283:2829-2836.
7. Cook RJ, Sackett DL. The number needed to treat: a clinically useful measure of treatment effect. *BMJ* 1995;310:452-454.
8. Tissue plasminogen activator for acute ischemic stroke. The National Institute of Neurological Disorders and Stroke rt-PA Stroke Study Group. *N Engl J Med* 1995;333:1581-1587.
9. Saver JL. Number needed to treat estimates incorporating effects over the entire range of clinical outcomes: novel derivation method and application to thrombolytic therapy for acute stroke. *Arch Neurol* 2004;61:1066-1070.
10. Saver JL. Hemorrhage after thrombolytic therapy for stroke: the clinically relevant number needed to harm. *Stroke* 2007;38:2279-2283.
11. Fierz W. Challenge of personalized health care: to what extent is medicine already individualized and what are the future trends? *Med Sci Monit* 2004;10:RA111-RA123.
12. Donnan GA, Davis SM. Neuroimaging, the ischaemic penumbra, and selection of patients for acute stroke therapy. *Lancet Neurol* 2002;1:417-425.
13. Tanne D, Bates VE, Verro P, Kasner SE, Binder JR, Patel SC, et al. Initial clinical experience with IV tissue plasminogen activator for acute ischemic stroke: a multicenter survey. The t-PA Stroke Survey Group. *Neurology* 1999;53:424-427.
14. Clark WM, Wissman S, Albers GW, Jhamandas JH, Madden KP, Hamilton S. Recombinant tissue-type plasminogen activator (Alteplase) for ischemic stroke 3 to 5 hours after symptom onset. The ATLANTIS Study: a randomized controlled trial. Alteplase Thrombolysis for Acute Noninterventional Therapy in Ischemic Stroke. *JAMA* 1999;282:2019-2026.
15. Hacke W, Donnan G, Fieschi C, Kaste M, von Kummer R, Broderick JP, et al. Association of outcome with early stroke treatment: pooled

analysis of ATLANTIS, ECASS, and NINDS rt-PA stroke trials. *Lancet* 2004;363:768-774.
16. Marler JR, Tilley BC, Lu M, Brott TG, Lyden PC, Grotta JC, et al. Early stroke treatment associated with better outcome: the NINDS rt-PA stroke study. *Neurology* 2000;55:1649-1655.
17. Adams HP Jr, del Zoppo G, Alberts MJ, Bhatt DL, Brass L, Furlan A, et al. Guidelines for the early management of adults with ischemic stroke: a guideline from the American Heart Association/American Stroke Association Stroke Council, Clinical Cardiology Council, Cardiovascular Radiology and Intervention Council, and the Atherosclerotic Peripheral Vascular Disease and Quality of Care Outcomes in Research Interdisciplinary Working Groups: the American Academy of Neurology affirms the value of this guideline as an educational tool for neurologists. *Stroke* 2007;38:1655-1711.
18. Lindsberg PJ, Häppölä O, Kallela M, Valanne L, Kuisma M, Kaste M. Door to thrombolysis: ER reorganization and reduced delays to acute stroke treatment. *Neurology* 2006;67:334-336.
19. Molina CA, Saver JL. Extending reperfusion therapy for acute ischemic stroke: emerging pharmacological, mechanical, and imaging strategies. *Stroke* 2005;36:2311-2320.
20. Heiss WD, Sobesky J, Smekal Uv, Dohmen C, Neveling M, Lackner K. Penumbra and irreversible damage in acute ischemic stroke: comparison of diffusion- and perfusion-weighted mangetic resonance imaging and positron emission tomography. *Ann Neurol* 2002;52:S24.
21. Darby DG, Barber PA, Gerraty RP, Desmond PM, Yang Q, Parsons M, et al. Pathophysiological topography of acute ischemia by combined diffusion-weighted and perfusion MRI. *Stroke* 1999;30:2043-2052.
22. Hacke W, Albers G, Al-Rawi Y, Bogousslavsky J, Davalos A, Eliasziw M, et al. The Desmoteplase in Acute Ischemic Stroke Trial (DIAS): a phase II MRI-based 9-hour window acute stroke thrombolysis trial with intravenous desmoteplase. *Stroke* 2005;36:66-73.
23. Furlan AJ, Eyding D, Albers GW, Al-Rawi Y, Lees KR, Rowley HA, et al. Dose Escalation of Desmoteplase for Acute Ischemic Stroke (DEDAS): evidence of safety and efficacy 3 to 9 hours after stroke onset. *Stroke* 2006;37:1227-1231.
24. Hjort N, Butcher K, Davis SM, Kidwell CS, Koroshetz WJ, Röther J, et al. Magnetic resonance imaging criteria for thrombolysis in acute cerebral infarct. *Stroke* 2005;36:388-397.
25. Köhrmann M, Jüttler E, Fiebach JB, Huttner HB, Siebert S, Schwark C, et al. MRI versus CT-based thrombolysis treatment within and beyond the 3 h time window after stroke onset: a cohort study. *Lancet Neurol* 2006;5:661-667.
26. Kidwell CS, Alger JR, Saver JL. Beyond mismatch: evolving paradigms in imaging the ischemic penumbra with multimodal magnetic resonance imaging. *Stroke* 2003;34:2729-2735.
27. Albers GW, Thijs VN, Wechsler L, Kemp S, Schlaug G, Skalabrin E, et al. Magnetic resonance imaging profiles predict clinical response to early reperfusion: the diffusion and perfusion imaging evaluation for understanding stroke evolution (DEFUSE) study. *Ann Neurol* 2006;60:508-517.
28. Olivot JM, Mlynash M, Thijs VN, Kemp S, Lansberg MG, Wechsler L, et al. Relationships between infarct growth, clinical outcome, and early recanalization in diffusion and perfusion imaging for understanding stroke evolution (DEFUSE). *Stroke* 2008;39:2257-2263.
29. Bang OY, Saver JL, Buck BH, Alger JR, Starkman S, Ovbiagele B, et al. Impact of collateral flow on tissue fate in acute ischaemic stroke. *J Neurology Neurosurg psychiatry* 2008;79:625-629.
30. Liebeskind DS. Collateral circulation. *Stroke* 2003;34:2279-2284.
31. Christoforidis GA, Mohammad Y, Kehagias D, Avutu B, Slivka AP. Angiographic assessment of pial collaterals as a prognostic indicator following intra-arterial thrombolysis for acute ischemic stroke. *AJNR Am J Neuroradiol* 2005;26:1789-1797.
32. Christensen S, Calamante F, Hjort N, Wu O, Blankholm AD, Desmond P, et al. Inferring origin of vascular supply from tracer arrival timing patterns using bolus tracking MRI. *J Magn Reson Imaging* 2008;27:1371-1381.
33. Bang OY, Saver JL, Alger JR, Starkman S, Ovbiagele B, Liebeskind DS; UCLA Collateral Investigators. Determinants of the distribution and severity of hypoperfusion in patients with ischemic stroke. *Neurology* 2008;71:1804-1811.
34. Kim SJ, Seok JM, Bang OY, Kim GM, Kim KH, Jeon P, et al. MR mismatch profiles in patients with intracranial atherosclerotic stroke: a comprehensive approach comparing stroke subtypes. *J Cereb Blood Flow Metab* 2009;29:1138-1145.
35. Heiss WD. Ischemic penumbra: evidence from functional imaging in man. *J Cereb Blood Flow Metab* 2000;20:1276-1293.
36. Tamura H, Hatazawa J, Toyoshima H, Shimosegawa E, Okudera T. Detection of deoxygenation-related signal change in acute ischemic stroke patients by T2*-weighted magnetic resonance imaging. *Stroke* 2002;33:967-971.
37. Baron JC, Bousser MG, Rey A, Guillard A, Comar D, Castaigne P. Reversal of focal "misery-perfusion syndrome" by extra-intracranial arterial bypass in hemodynamic cerebral ischemia. A case study with 15O positron emission tomography. *Stroke* 1981;12:454-459.
38. Hermier M, Nighoghossian N. Contribution of susceptibility-weighted imaging to acute stroke assessment. *Stroke* 2004;35:1989-1994.
39. Lee JM, Vo KD, An H, Celik A, Lee Y, Hsu CY, et al. Magnetic resonance cerebral metabolic rate of oxygen utilization in hyperacute stroke patients. *Ann Neurol* 2003;53:227-232.
40. Hermier M, Nighoghossian N, Derex L, Wiart M, Nemoz C, Berthezéne Y, et al. Hypointense leptomeningeal vessels at T2*-weighted MRI in acute ischemic stroke. *Neurology* 2005;65:652-653.
41. Roussel SA, van Bruggen N, King MD, Gadian DG. Identification of collaterally perfused areas following focal cerebral ischemia in the rat by comparison of gradient echo and diffusion-weighted MRI. *J Cereb Blood Flow Metab* 1995;15:578-586.
42. Gröhn OH, Lukkarinen JA, Oja JM, van Zijl PC, Ulatowski JA, Traystman RJ, et al. Noninvasive detection of cerebral hypoperfusion and reversible ischemia from reductions in the magnetic resonance imaging relaxation time, T2. *J Cereb Blood Flow Metab* 1998;18:911-920.
43. Ogawa S, Lee TM, Kay AR, Tank DW. Brain magnetic resonance imaging with contrast dependent on blood oxygenation. *Proc Natl Acad Sci U S A* 1990;87:9868-9872.
44. Geisler BS, Brandhoff F, Fiehler J, Saager C, Speck O, Röther J, et al. Blood-oxygen-level-dependent MRI allows metabolic description of tissue at risk in acute stroke patients. *Stroke* 2006;37:1778-1784.
45. Hermier M, Nighoghossian N, Derex L, Adeleine P, Wiart M, Berthezéne Y, et al. Hypointense transcerebral veins at T2*-weighted MRI: a marker of hemorrhagic transformation risk in patients treated with intravenous tissue plasminogen activator. *J Cereb Blood Flow Metab* 2003;23:1362-1370.
46. Marchal G, Beaudouin V, Rioux P, de la Sayette V, Le Doze F, Viader F, et al. Prolonged persistence of substantial volumes of potentially viable brain tissue after stroke: a correlative PET-CT study with voxel-based data analysis. *Stroke* 1996;27:599-606.
47. Kane I, Carpenter T, Chappell F, Rivers C, Armitage P, Sandercock P, et al. Comparison of 10 different magnetic resonance perfusion imaging processing methods in acute ischemic stroke: effect on lesion size, proportion of patients with diffusion/perfusion mismatch, clinical scores, and radiologic outcomes. *Stroke* 2007;38:3158-3164.
48. Wu O, Koroshetz WJ, Ostergaard L, Buonanno FS, Copen WA, Gonzalez RG, et al. Predicting tissue outcome in acute human cerebral ischemia using combined diffusion- and perfusion-weighted MR imaging. *Stroke* 2001;32:933-942.
49. Kakuda W, Lansberg MG, Thijs VN, Kemp SM, Bammer R, Wechsler LR, et al. Optimal definition for PWI/DWI mismatch in acute ischemic stroke patients. *J Cereb Blood Flow Metab* 2008;28:887-891.
50. Toth G, Albers GW. Use of MRI to Estimate the Therapeutic Window

in Acute Stroke: is perfusion-weighted imaging/diffusion-weighted imaging mismatch an EPITHET for salvageable ischemic brain tissue? *Stroke* 2009;40:333-335.
51. Kidwell CS, Chalela JA, Saver JL, Starkman S, Hill MD, Demchuk AM, et al. Comparison of MRI and CT for detection of acute intracerebral hemorrhage. *JAMA* 2004;292:1823-1830.
52. Singer OC, Humpich MC, Fiehler J, Albers GW, Lansberg MG, Kastrup A, et al. Risk for symptomatic intracerebral hemorrhage after thrombolysis assessed by diffusion-weighted magnetic resonance imaging. *Ann Neurol* 2008;63:52-60.
53. Selim M, Fink JN, Kumar S, Caplan LR, Horkan C, Chen Y, et al. Predictors of hemorrhagic transformation after intravenous recombinant tissue plasminogen activator: prognostic value of the initial apparent diffusion coefficient and diffusion-weighted lesion volume. *Stroke* 2002;33:2047-2052.
54. Alsop DC, Makovetskaya E, Kumar S, Selim M, Schlaug G. Markedly reduced apparent blood volume on bolus contrast magnetic resonance imaging as a predictor of hemorrhage after thrombolytic therapy for acute ischemic stroke. *Stroke* 2005;36:746-750.
55. Neumann-Haefelin T, Hoelig S, Berkefeld J, Fiehler J, Gass A, Humpich M, et al. Leukoaraiosis is a risk factor for symptomatic intracerebral hemorrhage after thrombolysis for acute stroke. *Stroke* 2006;37:2463-2466.
56. Kim EY, Na DG, Kim SS, Lee KH, Ryoo JW, Kim HK. Prediction of hemorrhagic transformation in acute ischemic stroke: role of diffusion-weighted imaging and early parenchymal enhancement. *AJNR Am J Neuroradiol* 2005;26:1050-1055.
57. Latour LL, Kang DW, Ezzeddine MA, Chalela JA, Warach S. Early blood-brain barrier disruption in human focal brain ischemia. *Ann Neurol* 2004;56:468-477.
58. Nagaraja TN, Nagesh V, Ewing JR, Whitton PA, Fenstermacher JD, Knight RA. Step-down infusions of Gd-DTPA yield greater contrast-enhanced magnetic resonance images of BBB damage in acute stroke than bolus injections. *Magn Reson Imaging* 2007;25:311-318.
59. Provenzale JM, Wang GR, Brenner T, Petrella JR, Sorensen AG. Comparison of permeability in high-grade and low-grade brain tumors using dynamic susceptibility contrast MR imaging. *AJR Am J Roentgenol* 2002;178:711-716.
60. Cha S, Yang L, Johnson G, Lai A, Chen MH, Tihan T, et al. Comparison of microvascular permeability measurements, K(trans), determined with conventional steady-state T1-weighted and first-pass T2*-weighted MR imaging methods in gliomas and meningiomas. *AJNR Am J Neuroradiol* 2006;27:409-417.
61. Kassner A, Roberts T, Taylor K, Silver F, Mikulis D. Prediction of hemorrhage in acute ischemic stroke using permeability MR imaging. *AJNR Am J Neuroradiol* 2005;26:2213-2217.
62. Bang OY, Buck BH, Saver JL, Alger JR, Yoon SR, Starkman S, et al. Prediction of hemorrhagic transformation after recanalization therapy using T2*-permeability magnetic resonance imaging. *Ann Neurol* 2007;62:170-176.
63. Lin K, Kazmi KS, Law M, Babb J, Peccerelli N, Pramanik BK. Measuring elevated microvascular permeability and predicting hemorrhagic transformation in acute ischemic stroke using first-pass dynamic perfusion CT imaging. *AJNR Am J Neuroradiol* 2007;28:1292-1298.
64. Bang OY, Saver JL, Alger JR, Shah SH, Buck BH, Starkman S, et al. Patterns and predictors of blood-brain barrier permeability derangements in acute ischemic stroke. *Stroke* 2009;40:454-461.
65. Lev MH. CT/NIHSS mismatch for detection of salvageable brain in acute stroke triage beyond the 3-hour time window: overrated or undervalued? *Stroke* 2007;38:2028-2029.
66. Hillis AE, Gold L, Kannan V, Cloutman L, Kleinman JT, Newhart M, et al. Site of the ischemic penumbra as a predictor of potential for recovery of functions. *Neurology* 2008;71:184-189.
67. Lee LJ, Kidwell CS, Alger J, Starkman S, Saver JL. Impact on stroke subtype diagnosis of early diffusion-weighted magnetic resonance imaging and magnetic resonance angiography. *Stroke* 2000;31:1081-1089.
68. Roh JK, Kang DW, Lee SH, Yoon BW, Chang KH. Significance of acute multiple brain infarction on diffusion-weighted imaging. *Stroke* 2000;31:688-694.
69. Bang OY, Lee PH, Heo KG, Joo US, Yoon SR, Kim SY. Specific DWI lesion patterns predict prognosis after acute ischaemic stroke within the MCA territory. *J Neurol Neurosurg Psychiatry* 2005;76:1222-1228.
70. Fisher M, Albers GW. Applications of diffusion-perfusion magnetic resonance imaging in acute ischemic stroke. *Neurology* 1999;52:1750-1756.
71. Kimura K, Minematsu K, Koga M, Arakawa R, Yasaka M, Yamagami H, et al. Microembolic signals and diffusion-weighted MR imaging abnormalities in acute ischemic stroke. *AJNR Am J Neuroradiol* 2001;22:1037-1042.
72. Lansberg MG, Thijs VN, O'Brien MW, Ali JO, de Crespigny AJ, Tong DC, et al. Evolution of apparent diffusion coefficient, diffusion-weighted, and T2-weighted signal intensity of acute stroke. *AJNR Am J Neuroradiol* 2001;22:637-644.
73. Sylaja PN, Coutts SB, Subramaniam S, Hill MD, Eliasziw M, Demchuk AM; VISION Study Group. Acute ischemic lesions of varying ages predict risk of ischemic events in stroke/TIA patients. *Neurology* 2007;68:415-419
74. Klein I, Iung B, Wolff M, Brochet E, Longuet P, Laissy JP, et al. Silent T2* cerebral microbleeds: a potential new imaging clue in infective endocarditis. *Neurology* 2007;68:2043.
75. Singhal AB, Topcuoglu MA, Buonanno FS. Acute ischemic stroke patterns in infective and nonbacterial thrombotic endocarditis: a diffusion-weighted magnetic resonance imaging study. *Stroke* 2002;33:1267-1273.
76. Jauss M, Wessels T, Trittmacher S, Allendörfer J, Kaps M. Embolic lesion pattern in stroke patients with patent foramen ovale compared with patients lacking an embolic source. *Stroke* 2006;37:2159-2161.
77. Hayashida K, Fukuchi K, Inubushi M, Fukushima K, Imakita S, Kimura K. Embolic distribution through patent foramen ovale demonstrated by (99m)Tc-MAA brain SPECT after Valsalva radionuclide venography. *J Nucl Med* 2001;42:859-863.
78. Bang OY, Heo JH, Kim JY, Park JH, Huh K. Middle cerebral artery stenosis is a major clinical determinant in striatocapsular small, deep infarction. *Arch Neurol* 2002;59:259-263.
79. Bang OY, Joo SY, Lee PH, Joo US, Lee JH, Joo IS, et al. The course of patients with lacunar infarcts and a parent arterial lesion: similarities to large artery vs small artery disease. *Arch Neurol* 2004;61:514-519.
80. Cho AH, Kang DW, Kwon SU, Kim JS. Is 15 mm size criterion for lacunar infarction still valid? A study on strictly subcortical middle cerebral artery territory infarction using diffusion-weighted MRI. *Cerebrovasc Dis* 2007;23:14-19.
81. Bang OY, Yeo SH, Yoon JH, Seok JI, Sheen SS, Yoon SR, et al. Clinical MRI cutoff points for predicting lacunar stroke may not exist: need for a grading rather than a dichotomizing system. *Cerebrovasc Dis* 2007;24:520-529.
82. Ay H, Furie KL, Singhal A, Smith WS, Sorensen AG, Koroshetz WJ. An evidence-based causative classification system for acute ischemic stroke. *Ann Neurol* 2005;58:688-697.
83. Cho ZH, Kang CK, Han JY, Kim SH, Kim KN, Hong SM, et al. Observation of the lenticulostriate arteries in the human brain in vivo using 7.0T MR angiography. *Stroke* 2008;39:1604-1606.
84. Jackson C, Sudlow C. Comparing risks of death and recurrent vascular events between lacunar and non-lacunar infarction. *Brain* 2005;128:2507-2517.
85. Kato H, Izumiyama M, Izumiyama K, Takahashi A, Itoyama Y. Silent cerebral microbleeds on T2*-weighted MRI: correlation with stroke subtype, stroke recurrence, and leukoaraiosis. *Stroke* 2002;33:1536-1540.

86. Briley-Saebo KC, Mulder WJ, Mani V, Hyafil F, Amirbekian V, Aguinaldo JG, et al. Magnetic resonance imaging of vulnerable atherosclerotic plaques: current imaging strategies and molecular imaging probes. *J Magn Reson Imaging* 2007;26:460-479.
87. Cai JM, Hatsukami TS, Ferguson MS, Small R, Polissar NL, Yuan C. Classification of human carotid atherosclerotic lesions with in vivo multicontrast magnetic resonance imaging. *Circulation* 2002;106:1368-1373.
88. Saam T, Ferguson MS, Yarnykh VL, Takaya N, Xu D, Polissar NL, et al. Quantitative evaluation of carotid plaque composition by in vivo MRI. *Arterioscler Thromb Vasc Biol* 2005;25:234-239.
89. Choudhury RP, Fuster V, Badimon JJ, Fisher EA, Fayad ZA. MRI and characterization of atherosclerotic plaque: emerging applications and molecular imaging. *Arterioscler Thromb Vasc Biol* 2002;22:1065-1074.
90. Sirol M, Itskovich VV, Mani V, Aguinaldo JG, Fallon JT, Misselwitz B, et al. Lipid-rich atherosclerotic plaques detected by gadofluorine-enhanced in vivo magnetic resonance imaging. *Circulation* 2004;109:2890-2896.
91. Kooi ME, Cappendijk VC, Cleutjens KB, Kessels AG, Kitslaar PJ, Borgers M, et al. Accumulation of ultrasmall superparamagnetic particles of iron oxide in human atherosclerotic plaques can be detected by in vivo magnetic resonance imaging. *Circulation* 2003;107:2453-2458.
92. Trivedi RA, Mallawarachi C, U-King-IM, Graves MJ, Horsley J, Goddard MJ, et al. Identifying inflamed carotid plaques using in vivo USPIO-enhanced MR imaging to label plaque macrophages. *Arterioscler Thromb Vasc Biol* 2006;26:1601-1606.
93. Malek AM, Alper SL, Izumo S. Hemodynamic shear stress and its role in atherosclerosis. *JAMA* 1999;282:2035-2042.
94. Fuster V, Moreno PR, Fayad ZA, Corti R, Badimon JJ. Atherothrombosis and high-risk plaque: part I: evolving concepts. *J Am Coll Cardiol* 2005;46:937-954.
95. Slager CJ, Wentzel JJ, Gijsen FJ, Thury A, van der Wal AC, Schaar JA, et al. The role of shear stress in the destabilization of vulnerable plaques and related therapeutic implications. *Nat Clin Pract Cardiovasc Med* 2005;2:456-464.
96. Groen HC, Gijsen FJ, van der Lugt A, Ferguson MS, Hatsukami TS, van der Steen AF, et al. Plaque rupture in the carotid artery is localized at the high shear stress region: a case report. *Stroke* 2007;38:2379-2381.
97. Chatzizisis YS, Coskun AU, Jonas M, Edelman ER, Feldman CL, Stone PH. Role of endothelial shear stress in the natural history of coronary atherosclerosis and vascular remodeling: molecular, cellular, and vascular behavior. *J Am Coll Cardiol* 2007;49:2379-2393.
98. Cebral JR, Castro MA, Burgess JE, Pergolizzi RS, Sheridan MJ, Putman CM. Characterization of cerebral aneurysms for assessing risk of rupture by using patient-specific computational hemodynamics models. *AJNR Am J Neuroradiol* 2005;26:2550-2559.
99. Glagov S, Zarins C, Giddens DP, Ku DN. Hemodynamics and atherosclerosis. Insights and perspectives gained from studies of human arteries. *Arch Pathol Lab Med* 1988;112:1018-1031
100. Zhao SZ, Ariff B, Long Q, Hughes AD, Thom SA, Stanton AV, et al. Inter-individual variations in wall shear stress and mechanical stress distributions at the carotid artery bifurcation of healthy humans. *J Biomech* 2002;35:1367-1377.
101. Papathanasopoulou P, Zhao S, Köhler U, Robertson MB, Long Q, Hoskins P, et al. MRI measurement of time-resolved wall shear stress vectors in a carotid bifurcation model, and comparison with CFD predictions. *J Magn Reson Imaging* 2003;17:153-162.
102. Lee SW, Antiga L, Spence JD, Steinman DA. Geometry of the carotid bifurcation predicts its exposure to disturbed flow. *Stroke* 2008;39:2341-2347.
103. Bang OY, Lee KH, Kim SJ, Liebeskind DS. Benign oligemia despite of a malignant MRI profile in acute ischemic stroke. *J Clin Neurol* 2009; In Press.
104. Bang OY. MRI for mismatch, deoxygenation, and blood-brainbarrier derangement in acute ischemic stroke. In: Liebeskind DS eds. *Therapeutic Strategies in Cerebral Ischemia. Oxford*, United Kingdom; Clinical publishing, In press.